5258 *Chem. Mater.* **2010,** *22,* 5258–5270
DOI:10.1021/cm101343j

CHEMISTRY OF MATERIALS
Article

Control of the Aggregation of a Phenylenevinylenediimide Chromophore by Use of Supramolecular Chemistry: Enhanced Electroluminescence in Supramolecular Organic Devices

Nicolas Delbosc,[†] Mathias Reynes,[†] Olivier J. Dautel,*[,†] Guillaume Wantz,[‡] Jean-Pierre Lère-Porte,[†] and Joël J. E. Moreau*[,†]

[†]*Architecture Moléculaire et Matériaux Nanostructurés, Instituts Charles Gerhardt Montpellier, Umr Cnrs 5253, Ecole Nationale Supérieure de Chimie de Montpellier, 8 rue de l'Ecole Normale 34296 Montpellier Cedex 05, France, and* [‡]*Laboratory IMS, Umr Cnrs 5218, Ecole Nationale Supérieure de Chimie et de Physique de Bordeaux, 16 Av. Pey Berland, 33607 Pessac Cedex, France*

Received May 12, 2010. Revised Manuscript Received July 13, 2010

A new approach toward the tuning of the supramolecular organization of π-conjugated substructures containing imide functional groups has been investigated using the concept of supramolecular chemistry. This approach, which allows enhanced emission properties of the active material, was evaluated in the fabrication of optoelectronic devices. A linear ditopic chromophore ***H*-ImPV** was synthesized. This N−H imide constitutes a recognizing unit with an acceptor−donor−acceptor (ADA) hydrogen bond motif. End-capping of this new chromophore with a monotopic structuring unit allowed control of the supramolecular aggregation of the π-conjugated chromophore. The studies of the absorption and emission properties of the ***H*-ImPV**, in solution or in the solid state (thin films, powders), clearly revealed different aggregation behaviors, depending on the presence of the monotopic structuring unit: hindered unit (***Cy*-DAT**) led to the formation of J-aggregates. In all cases, evidence for the heteromolecular association ***H*-ImPV···*Cy*-DAT** was obtained from an infrared absorption band located at 2715 cm^{-1}, which was typical of the hydrogen bonding present in the ADA···DAD triplet. This has been illustrated by the fabrication of light-emitting devices based on films of ***H*-ImPV** and [***H*-ImPV.(*Cy*-DAT)$_2$**]. ***H*-ImPV** presents a poor ability to emit light, because of its aggregation, which induces quenching of luminescence. The high efficiencies exhibited by the devices based on a single layer of [***H*-ImPV.(Cy-DAT)$_2$**] are the result of the *J*-aggregation of chromophores, because of the bulky cyclohexyl fragments of the ***Cy*-DAT**. Tuning of the supramolecular organization of the ***H*-ImPV** by the addition of two equivalents of ***Cy*-DAT** in the active layer allowed recovery of the performances exhibited by the organic light-emitting devices (OLEDs) of the isolated chromophore. Therefore, the use of ***Cy*-DAT** is an interesting alternative to avoid aggregation and to significantly increase luminance. As a consequence, the luminous efficiencies of the devices are much better for the coassembled active layer.

Introduction

The detailed understanding of the supramolecular interactions between the individual π-conjugated molecules has become a challenging scientific research area.[1] Recent strategies based on self-assembly and supramolecular chemistry are interesting alternatives for the bottom-up design of organic devices.[2,3] Controlled aggregation of π-conjugated systems offers interesting electronic and photonic functional materials that are different from their monomeric state. The self-association of chromophores in the solid or at the solid/liquid interface is a frequently encountered phenomenon in dye chemistry, because of strong intermolecular van der Waals-like attractive forces between molecules. The aggregates in the solid state exhibit distinct changes in the absorption band, compared to the monomeric species.[4] Thus, the aggregation pattern of π-conjugated oligomers will determine the device performance and/or goal, i.e., OLED or solar cells. In other words, it should be possible, using the same electroactive molecule, to tune its optoelectronic properties by simply playing on the modulation of its aggregation.

The tendency of molecules to aggregate and the nature of the supramolecular arrangement depend on the structure of the chromophore and also on its environment. However, the rational control of a dye aggregation is still difficult, because molecules tend to spontaneously align themselves into a one-dimensional infinite aggregate in a

*Author to whom correspondence should be addressed. E-mail addresses: joel.moreau@enscm.fr (J.J.E.M.), olivier.dautel@enscm.fr (O.J.D.).

(1) (a) Klaerner, G.; Mueller, M.; Morgenroth, F.; Wehmeier, M.; Soczka-Guth, T.; Muellen, K. *Synth. Met.* **1997**, *84*, 297. (b) Salzner, U. *Curr. Org. Chem.* **2004**, *8*, 569.
(2) Hoeben, F. J. M.; Jonkheijm, P.; Meijer, E. W.; Schenning, A. P. H. J. *Chem. Rev.* **2005**, *105*, 1491.
(3) Huang, C. H.; McClenaghan, N. D.; Kuhn, A.; Hofstraat, J. W.; Bassani, D. M. *Org. Lett.* **2005**, *7*, 3409.
(4) Mishra, A.; Behera, R. K.; Behera, P. K.; Mishra, B. K.; Behera, G. B. *Chem. Rev.* **2000**, *100*, 1973.

Published on Web 08/17/2010

Scheme 1. Cyclohexyle and Propyltriethoxysilyle End-Capped Bisimide Phenylenevinylene (*Cy*-ImPV and $(EtO)_3Si$-ImPV)

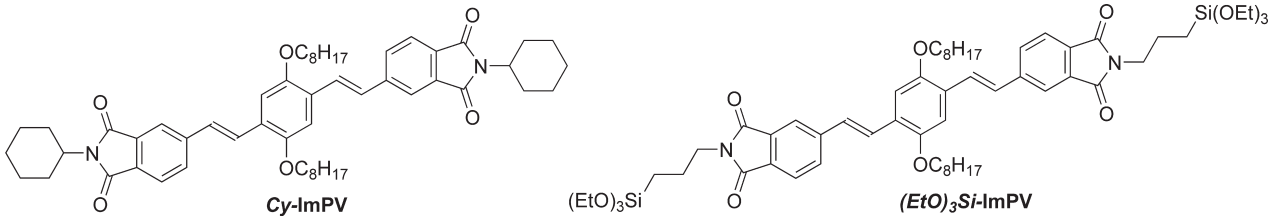

face-to-face manner by means of π-stacking and/or van der Waals interactions. The development of a method to control their aggregation behavior and orientations is a challenge.

As a result, we developed a new family of oligophenylenevinylene derivatives incorporating a conjugated imide phenylene vinylene (**ImPV**) substructure (***Cy*-ImPV** and **$(EtO)_3Si$-ImPV**; see Scheme 1).

The imide functions are thermally and chemically stable. Their electron affinity confers to the entire molecule the electron injection properties that are lacking to the phenylenevinylene moiety. The study of the relationship between the supramolecular organization of this novel bis-imido-phenylene vinylene (***Cy*-ImPV**) and its optoelectronic properties revealed that the good efficiencies exhibited by the devices based on a layer of ***Cy*-ImPV** were the result of the *J*-aggregation of chromophores in the material. It arose from the presence of bulky cyclohexyl fragments, which prevent card packing of the π-conjugated units.[5] Modifications of the aggregation state can allow a tuning of the optical properties. (Since the supramolecular organization of ***Cy*-ImPV** was the result of combined steric effects with π-stacking and van der Waals interactions, the only way to control it resides in the chemical modification of **ImPV**. This could be envisaged via the imide function. Indeed, any amine could be condensed to the 4-bromophthalic anhydride to furnish the reactive halogenated imide.) In a first approach, we explored the incorporation of the **ImPV** substructure in organosilica matrices, using the triethoxysilane function ($Si(OEt)_3$) (see Scheme 1: **$(EtO)_3Si$-ImPV**) as a modifiable bulky fragment.[6] After sol−gel hydrolysis, a change in the aggregation of the chromophore is observed, from *J*-aggregation to *H*-aggregation. The resulting material exhibited no more fluorescence but higher photoconductivity. However, chemical modification of the **ImPV** substructure is required to tune the molecular organization and control the properties for future applications. Sol−gel processing may lead to the same problems arising from the exposure of the devices to HCl vapors or from a premature hydrolysis/polycondensation of the sol containing the sol−gel precursor and a catalyst (H^+, OH^-, F^-).

We thought that a more interesting approach would result from the use of the concept of "supramolecular electronics", as defined by Meijer and Schenning.[7−9] The term "supramolecular electronics" refers to the formation of semiconducting networks of single or multicomponents, using the concept of supramolecular chemistry. The **ImPV** moiety represents an interesting building block to develop a new approach for controlling the supramolecular organization, using hydrogen bonding. Indeed, the presence of an imide function in ***H*-ImPV** gives, to this chromophore, the ability to act as both an hydrogen-bond donor and acceptor (see Scheme 2). In that case, N−H imides constitute a recognizing unit with the acceptor−donor−acceptor (ADA) hydrogen-bond sequence. As the complementary counterpart of this ADA sequence, a donor−acceptor−donor (DAD) unit is required. DAD subsequences are easily found in 2,4-diamino-1,3,5-triazine moiety (DAT). Therefore, the end-capping of the ***H*-ImPV** with DAT derivatives can bring different steric effects and should allow the control of its supramolecular aggregation. Here, we report the tuning of the aggregation properties of the ***H*-ImPV**, based on self-recognition with complementary units with different steric hindrance properties. Two derivatives of 2,4-diamino-1,3,5-triazine were selected: (i) the 6-cyclohexyl derivative ***Cy*-DAT**, which has a nonplanar aliphatic ring with a chair conformation, and (ii) the 6-phenyl planar derivative ***Ph*-DAT**,[10] which is of similar size to ***Cy*-DAT** but a different shape. Because of the different steric properties, *J*- or *H*-aggregation might be observed for ***Cy*-DAT** and ***Ph*-DAT**, respectively.

Results and Discussion

Synthesis. Linear ditopic chromophore ***H*-ImPV** was prepared in two steps, starting from 4-bromophthalic anhydride (**1**)[11] (see Scheme 3). Imidification of **1** in melt urea afforded 4-bromophthalimide (**2**). Finally, **2** readily underwent a coupling reaction with 1,4-divinyl-2,5-bis(octyloxy)benzene in the presence of a palladium catalyst to obtain the ditopic chromophore ***H*-ImPV**.

(5) Wantz, G.; Hirsch, L.; Vignau, L.; Parneix, J.-P.; Dautel, O. J.; Serein-Spirau, F.; Lère-Porte, J.-P.; Moreau, J. J. E.; Almairac, R. *Org. Electron.* **2005**, *7*, 38.
(6) Dautel, O. J.; Wantz, G.; Almairac, R.; Flot, D.; Hirsch, L.; Lère-Porte, J.-P.; Parneix, J. P.; Serein-Spirau, F.; Vignau, L.; Moreau, J. J. E. *J. Am. Chem. Soc.* **2006**, *128*, 4892.
(7) Meijer, E. W.; Schenning, A. P. H. J. *Nature* **2002**, *419*, 353.
(8) (a) Schenning, A. P. H. J.; Meijer, E. W. *Chem. Commun.* **2005**, 3245. (b) Hoeben, F. J. M.; Jonkheijm, P.; Meijer, E. W.; Schenning, A. P. H. J. *Chem. Rev.* **2005**, *105*, 1491.
(9) (a) Dautel, O. J.; Robitzer, M.; Lère-Porte, J.-P.; Serein-Spirau, F.; Moreau, J. J. E. *J. Am. Chem. Soc.* **2006**, *128*, 16213. (b) Dautel, O. J.; Robitzer, M.; Flores, J.-C.; Tondelier, D.; Serein-Spirau, F.; Lère-Porte, J.-P.; Guérin, D.; Lenfant, S.; Tillard, M.; Vuillaume, D.; Moreau, J. J. E. *Chem.—Eur. J.* **2008**, *14*, 4201.
(10) Diaz-Ortiz, A.; Elguero, J.; Foces-Foces, C.; de la Hoz, A.; Moreno, A.; del Carmen Mateo, M.; Sanchez-Migallon, A.; Valiente, G. *New J. Chem.* **2004**, *28*, 952–958.
(11) Dautel, O. J.; Wantz, G.; Flot, D.; Lère-Porte, J.-P.; Moreau, J. J. E.; Parneix, J.-P.; Serein-Spirau, F.; Vignau, L. *J. Mater. Chem.* **2005**, *15*, 4446.

Scheme 2. Molecular Model of (a) *H*-ImPV, (b) Supramolecule of *H*-ImPV End-Capped with *Cy*-DAT, and (c) Supramolecule of *H*-ImPV End-Capped with *Ph*-DAT and Expected Aggregation Type in the Solid State

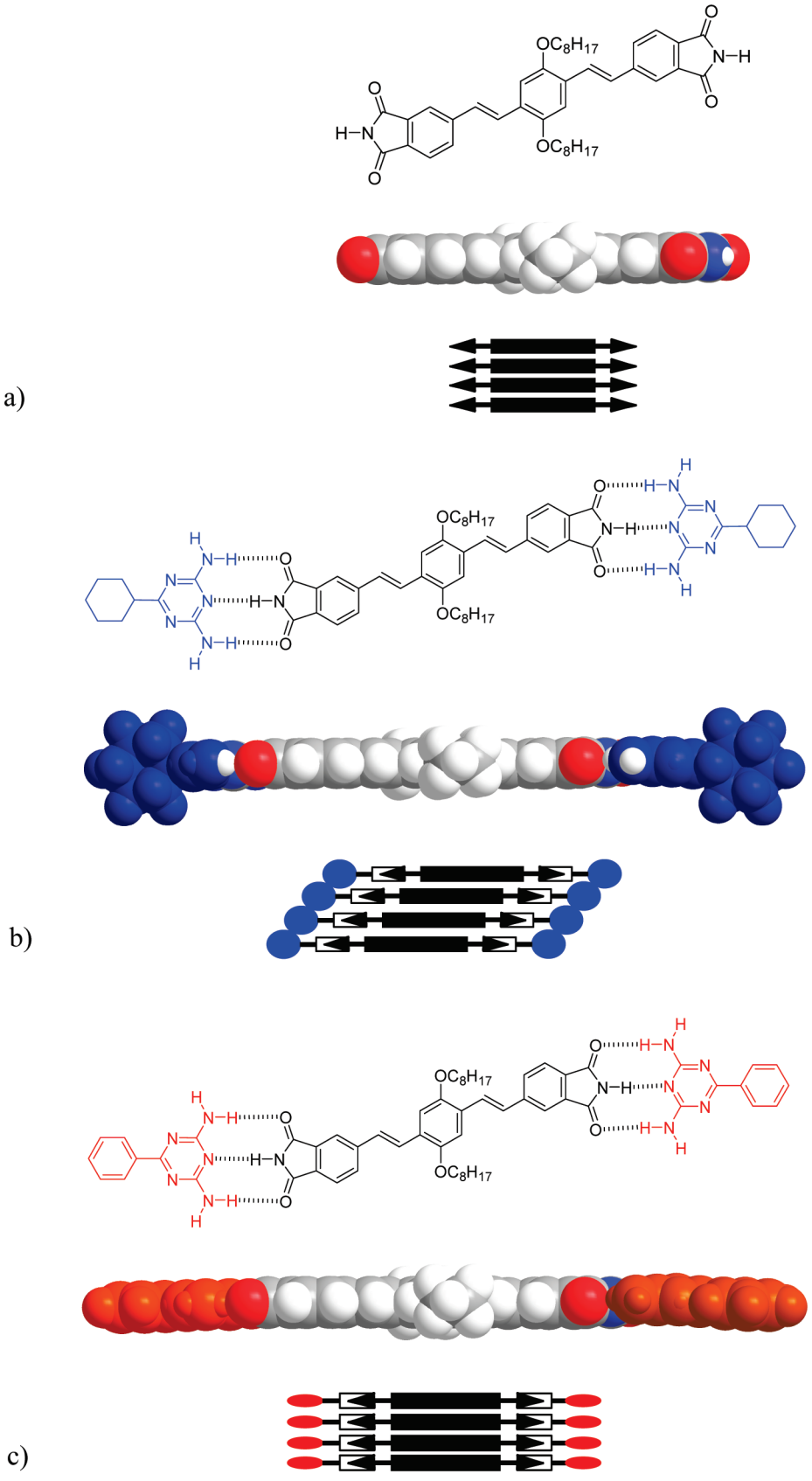

The Heck reaction was conducted in dry *N*,*N*-dimethylformamide at 90 °C in the presence of $Pd(OAc)_2$ and $P(o\text{-}C_6H_4Me)_3$.

Monotopic structuring modules ***Cy*-DAT** and ***Ph*-DAT** were synthesized from commercially available related cyano derivatives.[12] Cyclohexylcarbonitrile and benzonitrile react

Scheme 3. Steps for the Preparation of *H*-ImPV: (a) Urea, 160 °C, 2 h; (b) 1,4-Divinyl-2,5-bis(octyloxy)benzene, $Pd(OAc)_2$, $P(o\text{-}C_6H_4Me)_3$, NEt_3, DMF, 90 °C, 10 h

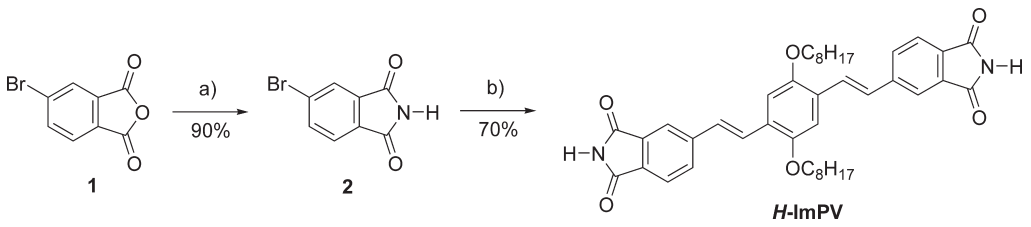

Chart 1. Structures of the Monotopic Structuring Modules, *Cy*-Dat, *Ph*-Dat, and *Cy*-DAT*Hex*$_4$

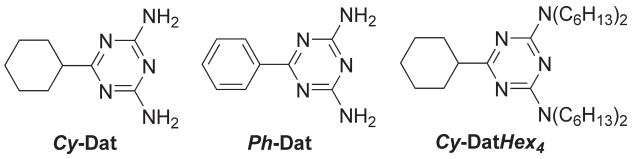

with dicyandiamide, under basic conditions at 150 °C, to afford phenyl-diaminotriazine (***Ph*-DAT**) and cyclohexyl-diaminotriazine (***Cy*-DAT**), respectively, in high yields. (Chart 1 shows their chemical structures.) Reference compound ***Cy*-DAT*Hex*$_4$**, which displays a structure similar to that of ***Cy*-DAT** but is incapable of establishing H-bond donating interactions, was obtained upon alkylation of the amine functions of ***Cy*-DAT** with an excess (5 equiv) of 1-bromohexane in the presence of 5 equiv of potassium *tert*-butoxide.

Control of the Aggregation of *H*-ImPV in Solution. While homodimers formed by AD···DA hydrogen bonding interactions may exist for ***H*-ImPV** molecules, heterotrimers (Scheme 2) will only be formed when the respective partners are mixed. Heterotrimers, resulting from self-assembly through triple hydrogen bonding, should be more stable than homodimers self-assembled through double hydrogen bonding.[13] Because of its low solubility in nonpolar solvents, attempts to determine the equilibrium self-association constant of ***H*-ImPV** by ^{1}H NMR were unsuccessful. However, using phthalimide (**IM**) as a model compound, self-association and inter-association constants with ***Cy*-DAT** or ***Ph*-DAT** could be measured in $CDCl_3$ (see Figures S11−S26 in the Supporting Information). The value of the equilibrium self-association constant for phthalimide (**IM**) was found to be very low (8.8 mol^{-1} L). In a same way, self-association constants of monotopic diaminotriazines are in the same order (8.9 mol^{-1} L and 23.8 mol^{-1} L for ***Cy*-DAT** and ***Ph*-DAT**, respectively), as reported by Beijer et al.[14] for the 2,4-diamino-6-*n*-dodecyl-s-triazine. Values of the inter-association constants of phthalimide with ***Cy*-DAT** or ***Ph*-DAT** (42 mol^{-1} L and 33.5 mol^{-1} L, respectively), were found to be higher in magnitude than the values of the self-association constants. Based on those constants, the formation of heterotrimers such as [***H*-ImPV**.(***Cy*-DAT**)$_2$] and [***H*-ImPV**.(***Ph*-DAT**)$_2$] must be favored in nonpolar solvents.

H*-ImPV** exhibits intense absorption bands in the UV region ($\lambda_{abs\text{-}max}$ = 430 nm) and is a strong luminophores ($\lambda_{em\text{-}max}$ = 510 nm) in polar solvents avoiding hydrogen bonds such as tetrahydrofuran (THF) with a fluorescence quantum yield of 46% using perylene as standard (Figure 1). The addition of 2 equiv of a monotopic structuring module (Cy*-DAT** or ***Ph*-DAT**) to a THF solution of ***H*-ImPV** (3×10^{-5} mol L^{-1}) exhibited no spectral changes, confirming that those monotopic modules have no influence on the optoelectronic properties of the ditopic chromophore. They will only play a role of structure directing agent without any electronic interaction with ***H*-ImPV**, such as charge transfer.

The absorption and fluorescence bands of ***H*-ImPV** in nonpolar solvents such as toluene or tetrachloroethylene (TCE) (5.9×10^{-5} M) exhibit fully reversible temperature-dependent profiles in the range of 25−60 °C (see Figure 2). The lower energy absorption band at 502 nm (not observed in THF) points to the presence of $\pi-\pi$ stacking interactions, most likely promoted by preliminary double H-bonds between ditopic chomophores.[15,16] Parallel to the changes in the absorption spectra, substantial variations of the fluorescence profiles occur when going from a polar solvent to the nonpolar solvent. The strong green fluorescence signal observed in THF (~500 nm) decreases by 90%, with a new maximum peak that appears at ~530 nm (see Figure 2b). These novel absorption and emission features of ***H*-ImPV** in nonpolar solvents are progressively lost upon increasing the temperature to 60 °C and are reversibly recovered by cooling the sample to 25 °C, also with the observation of a clean isosbestic point. These findings suggest that ***H*-ImPV** undergoes self-aggregation, which might be driven by a combination of weak homolecular hydrogen bonding, dipolar interactions, and $\pi-\pi$ stacking. We can reasonably assume that the terminal units of the linear ditopic module ***H*-ImPV** initially foster aggregation that further induces $\pi-\pi$ stacking.

(12) Iwakura, Y.; Uno, K.; Shiraishi, S. *Bull. Chem. Soc. Jpn.* **1965**, *38*, 1820.
(13) Würthner, F. *Chem. Commun.* **2004**, 1564.
(14) (a) Beijer, F. H.; Sijbesma, R. P.; Vekemans, J. A. J. M.; Meijer, E. W.; Kooijman, H.; Spek, A. L. *J. Org. Chem.* **1996**, *61*, 6371. (b) Krakovsky, I.; Lokaj, J.; Sedlakova, Z.; Ikeda, Y.; Nishida, K. *J. Appl. Polym. Sci.* **2006**, *101*, 2338.
(15) Kaiser, T. E.; Stepanenko, V.; Würthner, F. *J. Am. Chem. Soc.* **2009**, *131*, 6719.
(16) (a) Yoosaf, K.; Belbakra, A.; Armaroli, N.; Llanes-Pallas, A.; Bonifazi, D. *Chem. Commun.* **2009**, 2830. (b) Lanes-Pallas, A.; Palma, C.-A.; Piot, L.; Belbakra, A.; Listorti, A.; Prato, M.; Samori, P.; Armaroli, N.; Bonifazi, D. *J. Am. Chem. Soc.* **2009**, *131*, 509.

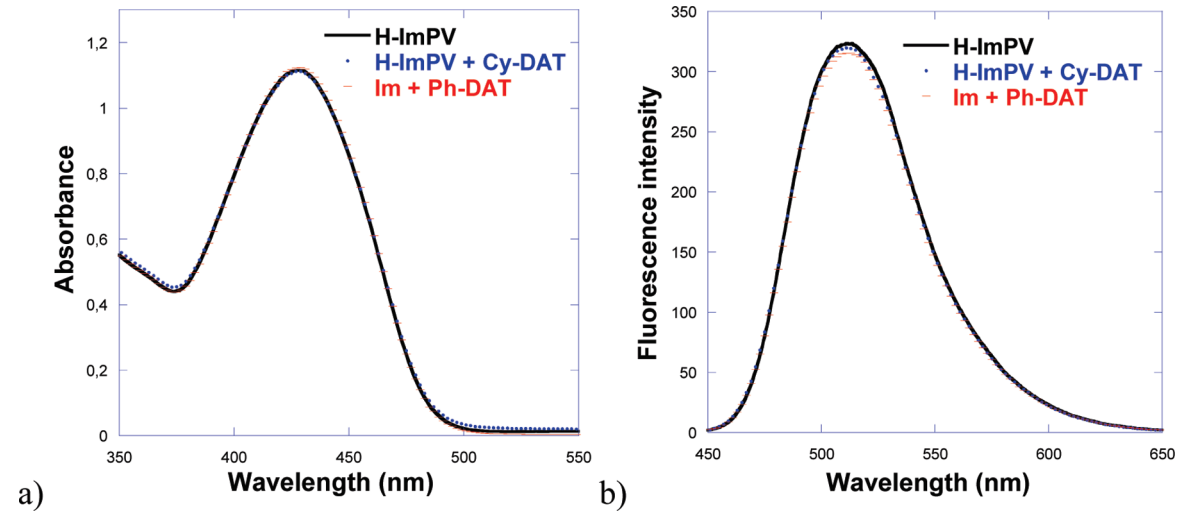

Figure 1. (a) UV−vis absorption spectra and (b) emission spectra (λ_{ex} = 430 nm) of ***H*-ImPV** (solid line), [***H*-ImPV.(*Cy*-DAT)$_2$**] in a 1:2 ratio (dotted line), and [***H*-ImPV.(*Ph*-DAT)$_2$**] (dashed line) in a 1:2 ratio in THF (3×10^{-5} mol L^{-1}).

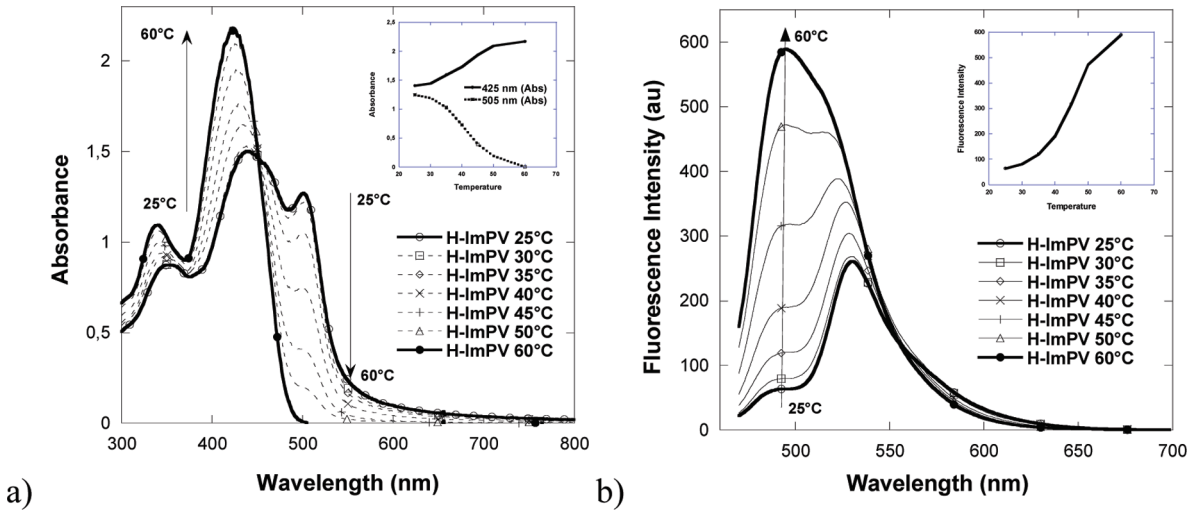

Figure 2. (a) UV−vis absorption spectra and (b) emission (spectra excitation at the isosbestic point λ_{ex} = 450 nm) of ***H*-ImPV** (5.9×10^{-5} mol L^{-1}) in toluene, as a function of the temperature.

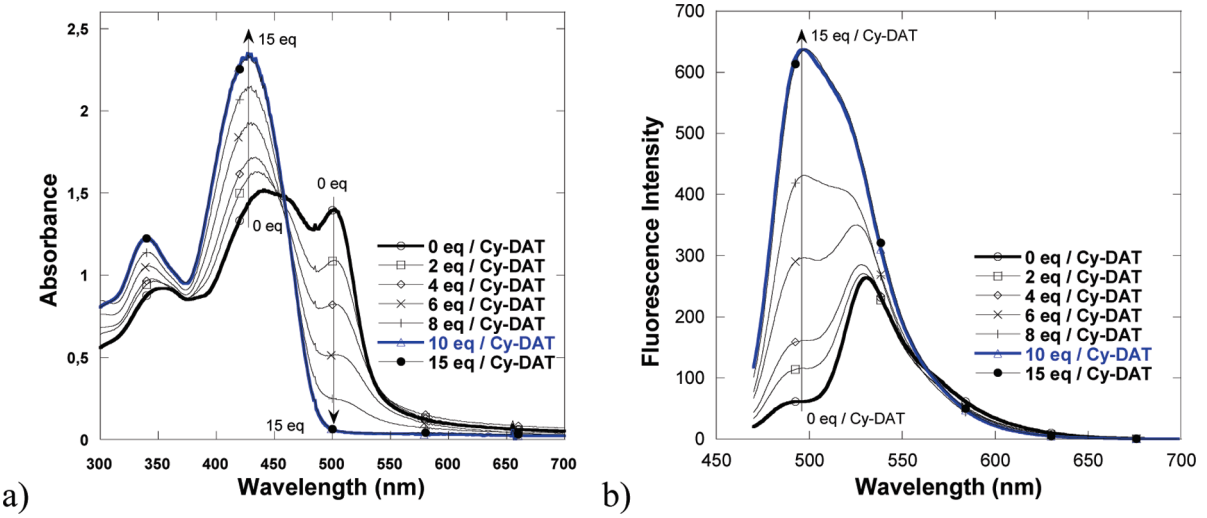

Figure 3. (a) UV−vis absorption spectra and (b) emission spectra (excitation at the isosbestic point, λ_{ex} = 455 nm) of ***H*-ImPV** (5.9×10^{-5} mol L^{-1}) in toluene at 25 °C with an increasing amount of ***Cy*-DAT**.

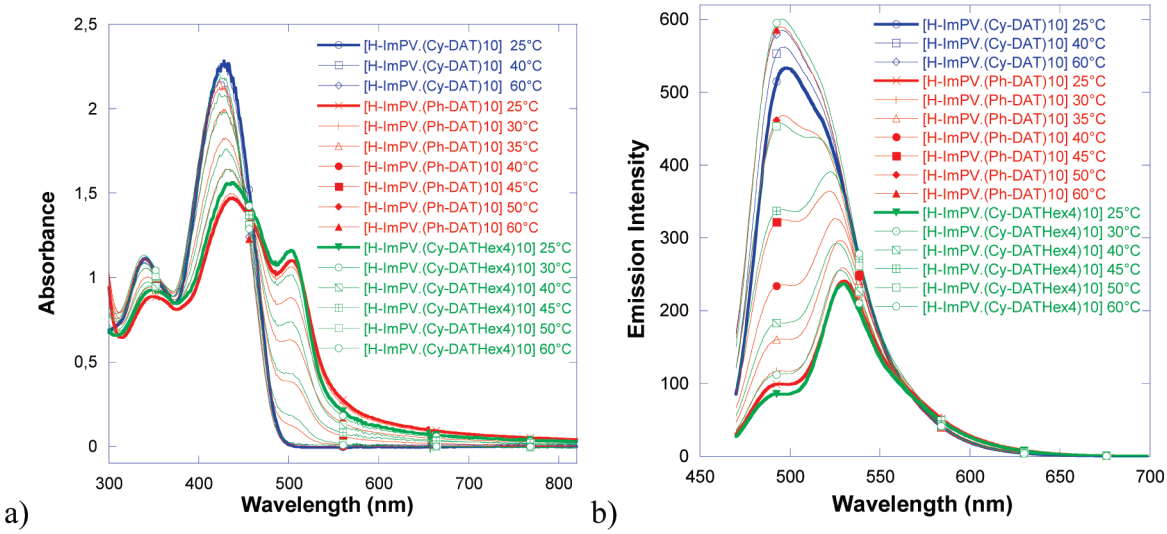

Figure 4. (a) UV−vis absorption spectra and (b) emission spectra (excitation at the isosbestic point λ_{ex} = 455 nm) of [***H*-ImPV.(*Cy*-DAT)$_{10}$**] (blue lines), [***H*-ImPV.(*Cy*-DAT*Hex*$_4$)$_{10}$**] (green lines), and [***H*-ImPV.(*Ph*-DAT)$_{10}$**] (red lines) in toluene (5.9×10^{-5} mol L^{-1}), as a function of the temperature.

The aggregation behavior of a mixture [***H*-ImPV.(*Cy*-DAT)$_x$**] in toluene turns out to be rather different from that obtained with ***H*-ImPV** itself (see Figure 3). The addition of an increasing amount of 6-cyclohexyl derivative ***Cy*-DAT**, which has a nonplanar ring, to the initial solution of ***H*-ImPV** in toluene allowed the formation of the aggregates to be controlled. Upon increasing the amount of ***Cy*-DAT**, the absorption band characteristic of the aggregated state of the ***H*-ImPV** progressively decreased (Figure 3a) while the strong green fluorescence signal of the free chromophore is also recovered (Figure 3b) with the observation of clean isosbestic and isoemissive points. Finally, the addition of 10 equiv was sufficient to avoid the aggregation of ***H*-ImPV**.

Once again, the supramolecular association of the two components is stable and reversible, as attested by the temperature-dependent experiments which evidence negligible spectral changes (see blue curves in Figures 4a and 4b). Using noncovalently bonded assemblies, we succeed in recovering the optical behavior of the **ImPV** covalently linked to a cyclohexyl fragment in ***Cy*-ImPV** (see Figure S27 in the Supporting Information). The rationale is supported by a control experiment carried out with ***Cy*-DAT*Hex*$_4$** (incapable of establishing hydrogen bonding interactions) and ***H*-ImPV**, where the experimental spectra exhibited the aggregation of ***H*-ImPV** (see green curves in Figure 4). This suggested that the suppression of the aggregation of the chromophore in the supramolecule [***H*-ImPV.(*Cy*-DAT)$_{10}$**] is most likely promoted by the preliminary formation of the triple H-bonds between complementary diaminotriazine and imide and not simply the result of the intercalation of the bulky fragment between the chromophores. In the same way, the nonplanar structure of the ***Cy*-DAT** proves to be essential to avoid aggregation through π-stacking interactions of the ***H*-ImPV**. End-capping of the ***H*-ImPV** with 10 equiv of the ***Ph*-DAT**, which is a planar monotopic module (see red curves in Figure 4) results in the self-aggregation of the trimolecule through $\pi-\pi$ stacking interactions. As anticipated from the molecular modelization, the phenyl substituent of the ***Ph*-DAT**, being in the plane of the π-conjugated chromophore (see Scheme 2), is not sufficient to avoid aggregation of the supramolecule resulting from its association with ***H*-ImPV**.

Even if we demonstrated that the aggregation behavior of the ***H*-ImPV** in solution could be tuned, in view of the fabrication of optoelectronic devices, this approach had to be transferred to the solid state. In solution, the addition of 10 equiv of a sterically hindered end-capper results in the formation of an isolated trimolecule. In this case, the issue involves solubilization of the chromophore through the formation of a soluble supramolecule. No specific interaction could be observed between the [***H*-ImPV.(*Cy*-DAT)$_x$**] supramolecules in the solution. However, while going from the solution to the solid, those supramolecules should interact between each other. In this case, the ***Cy*-DAT** should drive the supramolecular organization of the trimolecules toward a *J*-aggregation. This organization usually results in modification of the spectroscopic behavior of the material (red shift of the absorption maximum and strong fluorescence emission).

Control of the Optoelectronic Properties of *H*-ImPV in the Solid State. In a first approach, study of the aggregation behavior of ***H*-ImPV** was realized on thin films (Figure 5). Surprisingly, the UV−vis absorption spectra of thin films obtained from the spin coating of THF solutions (3×10^{-3} mol L^{-1}) of ***H*-ImPV**, [***H*-ImPV.(*Ph*-DAT)$_2$**] or [***H*-ImPV.(*Cy*-DAT)$_2$**] exhibited the same spectral modifications. In all cases, the strong absorption of the chromophore observed at 430 nm in THF is dramatically red-shifted by ~50 nm to be located at 489, 485, and 493 nm, respectively (see Figure 5a). However, study of the emission properties of the different films revealed different aggregation behaviors. Interestingly, spin coating of those solutions on glass substrates revealed that the emission properties were extremely enhanced by the addition of the cyclohexyl function (see

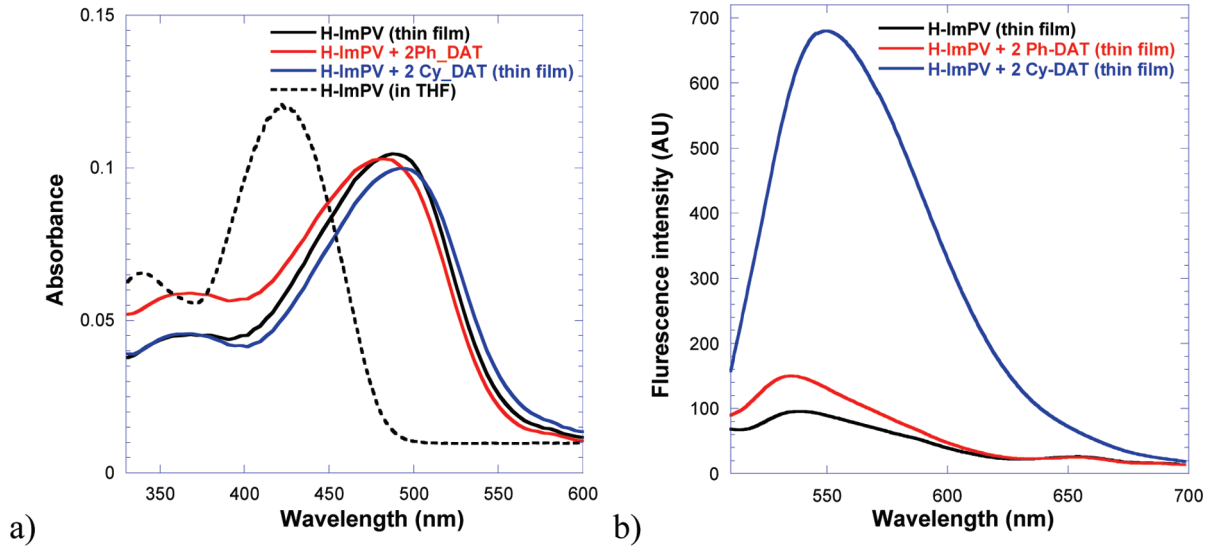

Figure 5. (a) UV−vis absorption spectra and (b) emission spectra of thin films obtained from the spin coating of THF solutions (3×10^{-3} mol L^{-1}) of ***H*-ImPV** (black curve), [***H*-ImPV.(*Ph*-DAT)$_2$]** (red curve), and [***H*-ImPV.(*Cy*-DAT)$_2$]** (blue curve) on glass plates. The absorption spectrum of the ***H*-ImPV** in THF is added as a dotted line.

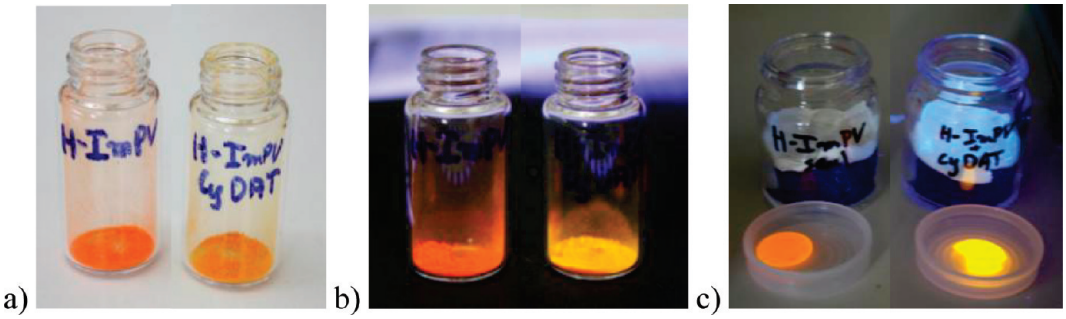

Figure 6. Pictures of ***H*-ImPV** (left) and [***H*-ImPV.(*Cy*-DAT)$_2$]** (right) powders obtained from the recrystallization of the ***H*-ImPV** in dioxane in the absence (or presence) of 4 equiv of ***Cy*-DAT**: (a) observed in the daylight, (b) observed under a 365-nm excitation, and (c) diluted in KBr under a 365-nm irradiation.

Figure 5b). A film of [***H*-ImPV.(*Cy*-DAT)$_2$]** is 1 order of magnitude more fluorescent than a film composed of ***H*-ImPV**. One could consider that it is simply a dilution of the ***H*-ImPV** in the ***Cy*-DAT**. However, using ***Ph*-DAT** instead of ***Cy*-DAT**, the ***Ph*-DAT**, being less hindered, shows no improvement in the fluorescence properties of the films. Two equivalents of ***Cy*-DAT** were sufficient to optimize the fluorescence properties of the films. Increasing the amount of ***Cy*-DAT** results in a decrease in the fluorescence intensity of the thin film (see Figure S28 in the Supporting Information). Again, this suggested that the suppression of the aggregation of the chromophore in the supramolecule [***H*-ImPV.(*Cy*-DAT)$_2$]** is most likely promoted by the preliminary formation of the triple H-bonds between complementary diaminotriazine and imide and not simply the result of the intercalation of the bulky fragment between the chromophores. These studies of the absorption and emission properties of the different films clearly revealed different aggregation behaviors. Indeed, in the case of a *Foster* aggregation[16] that further induces $\pi-\pi$ stacking, as in the case of a J-aggregation, one can observe a red-shift of the absorption spectra; however, the dipole configuration of a *J*-aggregates prevents fluorescence quenching, unlike that observed for *Foster* aggregates.

In a related approach, heteromolecular microcrystalline powders could be fabricated through the recrystallization of the ***H*-ImPV** in dioxane in the absence (or presence) of 4 equiv of ***Cy*-DAT**. The powders were obtained from the slow cooling (0.2 °C/h) of dioxane solutions preheated at 70 °C. Filtration of the resulting material yielded a red powder in the case of the ***H*-ImPV** and a yellow powder in the case of the heteromolecular material (***H*-ImPV** + ***Cy*-DAT**) (see Figure 6).

The ratio between the ***H*-ImPV** and the ***Cy*-DAT** hosted in the material could be determined by ^{1}H NMR analysis (see Figure S30 in the Supporting Information) and TGA (see Figure S31 in the Supporting Information) analysis of the powders. In good agreement with the conclusions reached from the study of the emission properties of thin films giving a 2:1 optimum ratio, both analyses resulted in the same formulation.

Again, the [***H*-ImPV.(*Cy*-DAT)$_2$]** powder exhibited much higher emitting properties than that of ***H*-ImPV** (see Figures 6b and 6c). As an example, the fluorescence intensity of KBr disks containing 2 wt % of [***H*-ImPV.(*Cy*-DAT)$_2$]** powder is 1 order of magnitude more intense than that of ***H*-ImPV**. (See Figure S29 in the Supporting Information.) The better emitting properties of the [***H*-ImPV.(*Cy*-DAT)$_2$]** powder could be quantified by the

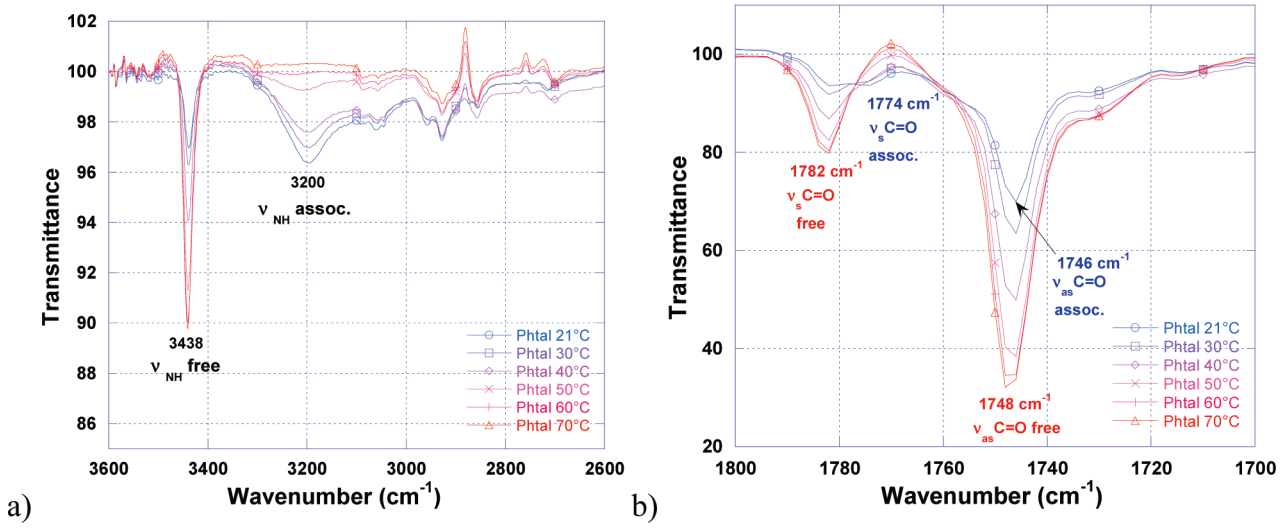

Figure 7. Fourier transform infrared (FT-IR) spectra of a 10 mM solution of phthalimide (**IM**) in tetrachloroethylene (TCE), as a function of the temperature in the region of (a) $N-H_{imide}$ stretching and (b) C═O stretching.

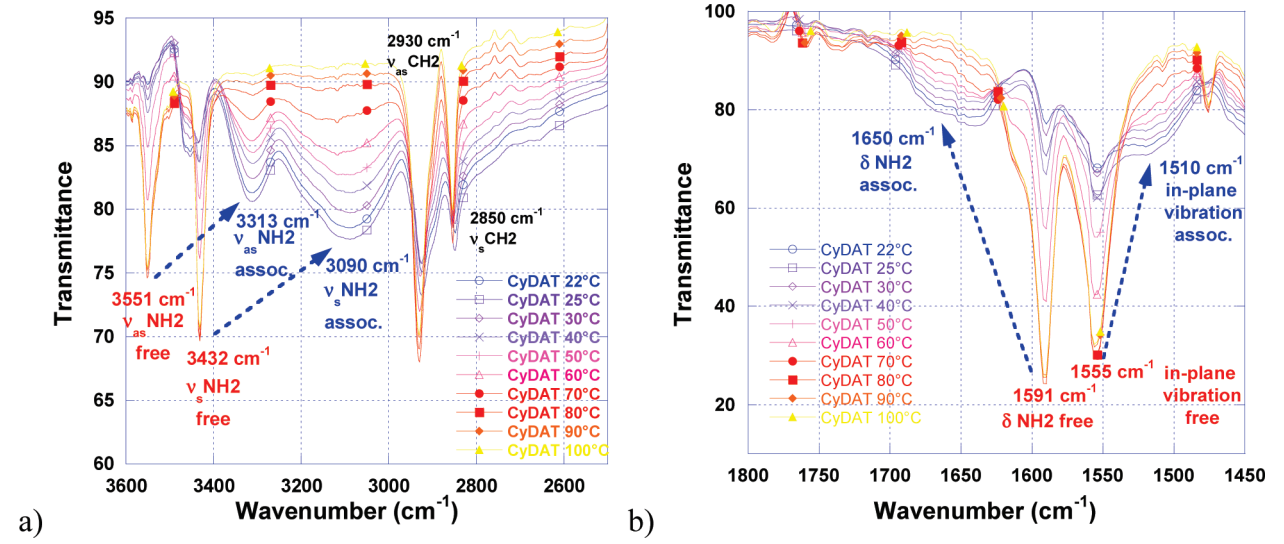

Figure 8. FT-IR spectra of a 10 mM solution of ***Cy*-DAT** in TCE, as a function of the temperature in the region of (a) NH_{amine} stretching and (b) NH_{amine} bending and triazine ring.

determination of its absolute emission quantum yield (ϕ). The quantum yields (ϕ) were measured at room temperature using a quantum yield measurement system (Hamamatsu, Model C9920-02) with a 150-W xenon lamp coupled to a monochromator for wavelength discrimination, an integrating sphere as the sample chamber, and a multichannel analyzer for signal detection. In this case, the heteromolecular material exhibited a much higher absolute quantum yield ($\phi_{[H\text{-ImPV}\cdot(Cy\text{-DAT})_2]}$ = 37%) than that of the homomolecular material ($\phi_{H\text{-ImPV}}$ = 14%).

FTIR Evaluation of the Hydrogen Bonding. Results from the optical properties of the films or the powders do not give information about ***H*-ImPV···*Cy*-DAT** interaction, i.e., if the role of DATs consists only in breaking ***H*-ImPV···*H*-ImPV** hydrogen bonds (inert plasticizer) or new hydrogen bonds between ***H*-ImPV** and ***Cy*-DAT** are formed in an ADA···DAD triplet. Such information may be provided by infrared spectroscopy. In the case of ***H*-ImPV···*Cy*-DAT** interaction, new types of hydrogen bonding not present in phthalimide or DAT themselves may be manifested in the spectra of the mixture. However, to differentiate bands of new $N-H_{amine}\cdots O{=}C$, new $N-H_{imide}\cdots O{=}C$, new $N-H_{imide}\cdots N_{amine}$ and new $N-H_{amine}\cdots N_{amine}$, respectively, is a very difficult task. With this intention, our strategy was to study first a simple model. In this case, it will concern the association of phthalimide (**IM**) and ***Cy*-DAT** (see Figures 7, 8, and 9). Moreover, the study was carried out on solutions in TCE, as a function of the temperature. It is easier to follow the evolution of a band in terms of shape and wavenumber as a function of the temperature than to compare steady state. At high temperature, species appear as free molecules and with the reduction in temperature, homomolecular or heteromolecular association will produce FTIR spectral modifications. As a consequence, experiments were performed in a screw-sealed cell built from two slices of crystalline KBr (see Figure S32 in the Supporting Information).

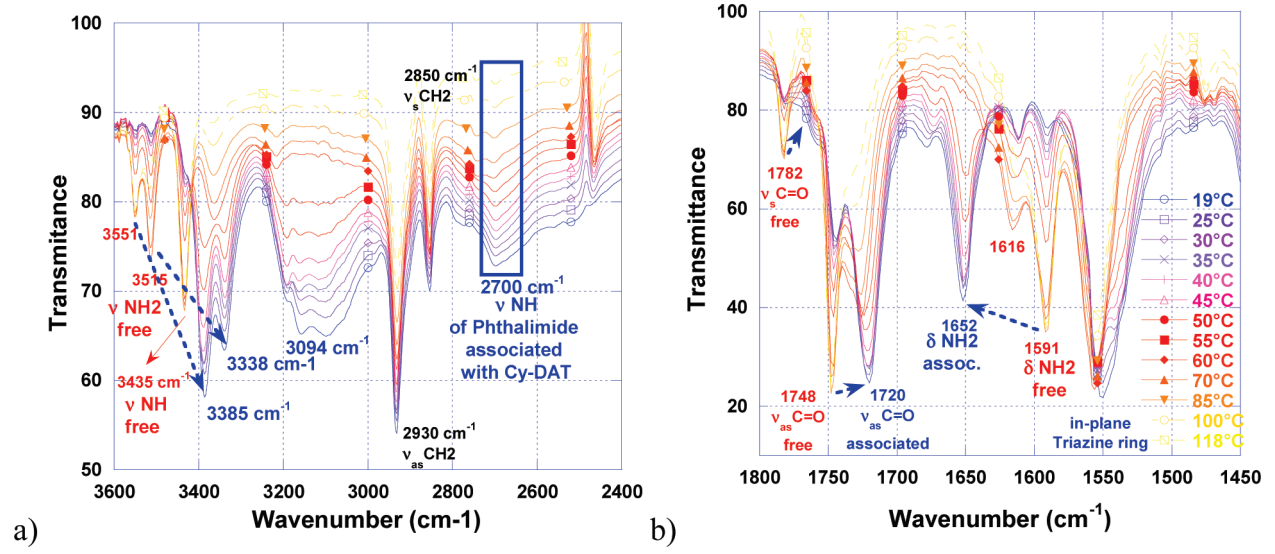

Figure 9. FT-IR spectra of a 10 mM solution of **IM:*Cy*-DAT** in 1:1 ratio in TCE, as a function of the temperature in the region of (a) N−H_{imide} stretching and N−H_{amine} stretching and (b) C═O stretching, N−H_{amine} bending and triazine ring.

The control of the temperature was ensured by the application of a bias on a resistance enveloping the cell.

In a first step, both modules have been studied separately, to identify the modification of the IR absorption resulting from their homoassociations. Finally, the study of the mixture in a 1:1 ratio pointed out spectral modifications resulting from the heteroassociations. A particular attention has been paid to the N−H_{imide} and C═O stretching of **IM** and N−H_{amine} stretching of ***Cy*-DAT**. Two regions important for the investigation of hydrogen bonding, N−H_{imide} stretching (3600−2400 cm^{-1}) and C═O stretching (1800−1650 cm^{-1}) in spectra obtained from the phthalimide **IM** used in our study are shown in Figure S33 in the Supporting Information. In accordance with interpretation given by Krakovsky et al.,[17] a broad band centered at ~3200 cm^{-1} (see Figure 7a) was assigned to a wide distribution of hydrogen bonded structures (multimers) resulting from the homoassociation of **IM**. The sharp band at 3438 cm^{-1} was attributed to free **IM** units. Similarly, two bands shown in Figure 7b—a smaller band centered at 1775 cm^{-1} and the bigger one at ca. 1748 cm^{-1}, respectively—can be attributed to the C═O stretching which is either in-phase (ν_s(C═O)) or out-of-phase (ν_{as}(C═O)) vibrations with the **IM** ring. Those two bands are almost unchanged upon cooling.

Spectra of ***Cy*-DAT** in TCE, as a function of the temperature, were measured and reported in Figure 8.[18] Two main regions of the infrared absorption were found: 1450−1800 cm^{-1} and 2550−3600 cm^{-1}. The first region contains, at high temperature, two sharp peaks, at 1591 cm^{-1} and 1555 cm^{-1}, which were respectively assigned to bending of the NH_2 ($\delta(NH_{amine})$) and the in-plane vibration of the triazine ring of the free triazine (see Figure 8b). Upon cooling, both bands are broadened. The NH_2 bending is shifted to higher wavenumbers (1640 cm^{-1}) and the in-plane vibration of the triazine ring is shifted to lower wavenumbers (1510 cm^{-1}). In the same way, the second region (Figure 8a) contains two absorptions bands of asymmetric $\nu_{as}(NH_{amine})$ and symmetric $\nu_s(NH_{amine})$ stretching at ca. 3551 and 3432 cm^{-1}, corresponding to the free DAT. Upon cooling, both sharp peaks are broadened and shifted to lower frequencies and could be attributed to the homoassociated DAT.

Spectra obtained from the 1:1 **IM**:***Cy*-DAT** mixture are more complex; nevertheless, a few conclusions can be made (see Figure 9). At high temperature, both components are free and the spectrum of the mixture results from the addition of the spectra of the individual modules. The two broad bands at 1640 cm^{-1} and 1510 cm^{-1} assigned to bending of the NH_2 ($\delta(NH_{amine})$) and the in-plane vibration of the triazine ring of the homoassociated triazine (observed in Figure 8b), are in the mixture converted to two sharp peaks, at 1652 cm^{-1} and 1550 cm^{-1} (see Figure 9b). This observation can be interpreted as an indication of the participation of NH_2 from DAT in a new type of well-defined hydrogen-bonding pattern occurring in the heteroassociated triplet. In a same way, the two absorptions bands of asymmetric $\nu_{as}(NH_{amine})$ and symmetric $\nu_s(NH_{amine})$ stretching at ca. 3551 and 3432 cm^{-1}, corresponding to the free DAT, are in the mixture converted to a sharp doublet at 3385 cm^{-1} and 3338 cm^{-1}. Similarly, the position of the asymmetric stretching of the free imide (ν_{as}(C═O)), which was almost unchanged upon cooling (recall Figure 7b), is shifted to lower frequencies at 1720 cm^{-1} by the presence of the DAT.[19] The signature of the heteromolecular association is given by the band at 2700 cm^{-1} in Figure 9a, which is typical of the hydrogen bonding present in the ADA···DAD triplet. This broad infrared absorption must be attributed the central N−H···N hydrogen bond involving the NH group of the imide and the ring nitrogen in position 3 of

(17) Krakovsky, I.; Lokaj, J.; Sedlakova, Z.; Ikeda, Y.; Nishida, K. *J. Appl. Polym. Sci.* **2006**, *101*, 2338.
(18) Padgett, W. M., II; Hammer, W. F. *J. Am. Chem. Soc.* **1958**, *80*, 803.
(19) Musto, P.; Karasz, F. E.; MacKnight, W. J. *Macromolecules* **1991**, *24*, 4762.

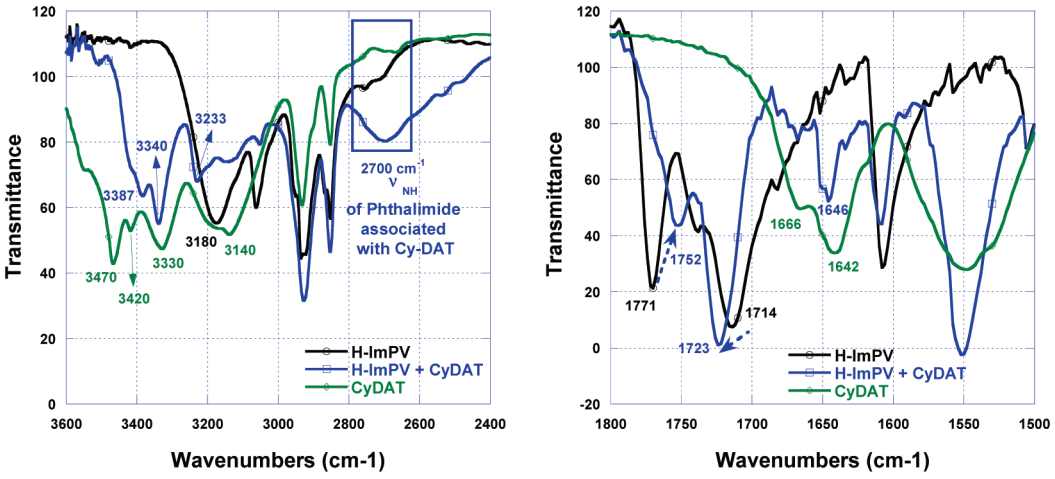

Figure 10. FTIR spectra realized on KBr pellets containing 2 wt % of **Cy-DAT** (green line), **H-ImPV** (black line) and [***H*-ImPV.(*Cy*-DAT)$_2$**] powder (blue line) in the region of (a) N−H$_{imide}$ stretching and N−H$_{amine}$ stretching and (b) C=O stretching, N−H$_{amine}$ bending and triazine ring.

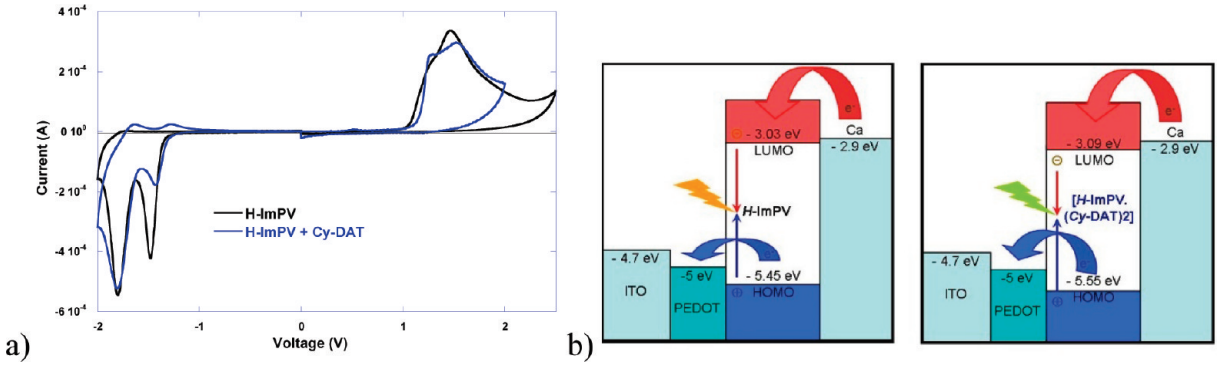

Figure 11. (a) Cyclic voltammograms of drop-cast films from THF solution of ***H*-ImPV** (black line) and [***H*-ImPV.(*Cy*-DAT)$_2$**] (blue line) on platinum wires in CH_3CN containing 0.1 mol L^{-1} of Bu_4NPF_6 as a supporting electrolyte at a scan rate of 100 mV s^{-1}, referenced vs SCE. (b) Energy level diagram of the organic light-emitting diodes (OLEDs) fabricated with evaporated films of ***H*-ImPV** or [***H*-ImPV.(*Cy*-DAT)$_2$**] (before contact).

the triazine.[20] This type of N−H···N interaction is much stronger than the N−H···O interaction, which implies that the equilibrium constant describing inter-association has greater value than that describing self-association.[21]

In view of the above conclusions and observations given by the study of the model, we were able to evidence the heteroassociation of the ***H*-ImPV** and ***Cy*-DAT** in the powder and in the films (see Figure 10).

FT-IR measurements realized on KBr pellets containing 2 wt % **Cy-DAT** (green line), **H-ImPV** (black line) and [***H*-ImPV.(*Cy*-DAT)$_2$**] (blue line) confirmed the contribution of the imide group to the formation of heteromolecular association. The infrared spectrum of [***H*-ImPV.(Cy-DAT)$_2$**], relative to ***H*-ImPV**, exhibited both shifting of the symmetric ν_s(C=O) stretching to lower wavenumber ($\Delta\nu$ = −9 cm^{-1}) and shifting of the asymmetric ν_{as}(C=O) and ($\Delta\nu$ = 19 cm^{-1}) (see Figure 10b). Those shifts are indicative of a more-effective hydrogen bond in the triplet ADA···DAD. The band at ca. 2715 cm^{-1}, which is assigned to the N−H···N interassociation of ***Cy*-DAT** and ***H*-ImPV** units, is again clearly seen in the spectrum of the [***H*-ImPV.(Cy-DAT)$_2$**] powder shown in Figure 10a.

Enhanced Electroluminescence in Hydrogen-Bonded All-Organic Devices Based on *H*-ImPV. To gain information on the charge injection, electrochemical measurements were performed. Figure 11a shows full scan cyclic voltammograms for thin films of ***H*-ImPV** and [***H*-ImPV.(*Cy*-DAT)$_2$**] drop-cast on a platinum wire. Both compounds exhibit two irreversible waves under cathodic sweep and the reduction occurred, respectively, at −1.37 V (E_{LUMO} = −3.03 eV) and −1.31 V (E_{LUMO} = −3.09 eV) versus saturated calomel electrode (vs SCE).

The oxidation process exhibits an irreversible wave when swept anodically, and the onset potential of oxidation for ***H*-ImPV** is located at 1.05 V (E_{HOMO} = −5.45 eV) vs SCE. [***H*-ImPV.(*Cy*-DAT)$_2$**] exhibits a higher oxidation potential at 1.15 V (E_{HOMO} = −5.55 eV). It is easier to inject holes in the HOMO of ***H*-ImPV** than that of [***H*-ImPV.(*Cy*-DAT)$_2$**]. The supramolecular aggregation of ***H*-ImPV** optimizes the π-orbital overlap between chromophores and thus should improve its charge-transport ability. These values of the oxidation potential showed that the *J*-type aggregation of [***H*-ImPV.(*Cy*-DAT)$_2$**] is more effective than that of ***Cy*-ImPV**. Indeed,

(20) Bishop, M. M.; Lindoy, L. F.; Skelton, B. W.; White, A. H. *J. Chem. Soc., Dalton Trans.* **2002**, 377.
(21) Vermeesch, I. M.; Groeninckx, G.; Coleman, M. M. *Macromolecules* **1993**, *26*, 6643.

the oxidation potential of ***Cy*-ImPV** (1.07 V, see ref 6) resides between that of ***H*-ImPV** (1.05 V) and [***H*-ImPV.(*Cy*-DAT)$_2$**] (1.15 V) values. Similarly, good correlation could be achieved with the study that we recently reported,[5] regarding the influence of the sol−gel process on the optoelectronic properties of **(*EtO*)$_3$*Si*-ImPV**. **(*OEt*)$_3$*Si*-ImPV**, in a J-aggregation before the sol−gel process, exhibits a higher oxidation potential at 1.18 V (lower hole injection ability) than the chromophore embedded in the sol−gel material **(*O*)$_{1.5}$*Si*-ImPV** with an oxidation potential of 1.0 V. The supramolecular reorganization optimizes the overlap between chromophores during the sol−gel process and improves the hole transport ability of the material. Finally, the supramolecular organization of the supramolecule [***H*-ImPV.(*Cy*-DAT)$_2$**], E_{ox} = 1.15 V vs SCE) is closely related to the J-aggregation of the sol−gel precursor [**(*EtO*)$_3$*Si*-ImPV**, E_{ox} = 1.18 V vs SCE] and ***H*-ImPV** (E_{ox} = 1.05 V vs SCE) behaves as the sol−gel material in an H-aggregation [**(*O*)$_{1.5}$*Si*-ImPV**, E_{ox} = 1.0 V vs SCE]. The electrochemical bandgaps (E_g^{EC}), calculated from cyclic voltammetry data ($E_{on}^{ox} - E_{on}^{red}$), are ∼2.42 eV for ***H*-ImPV** and 2.46 eV for [***H*-ImPV.(*Cy*-DAT)$_2$**], in somewhat good accordance with the optical bandgap (E_g^{opt}) estimated from the onset absorption of thin film of ***H*-ImPV** (2.25 eV, λ_{onset} = 551 nm) and [***H*-ImPV.(*Cy*-DAT)$_2$**] (2.25 eV, λ_{onset} = 549 nm).

According to the experimental data given by UV−visible spectroscopies (absorption and emission) and electrochemical measurements, ***H*-ImPV** and [***H*-ImPV.(*Cy*-DAT)$_2$**], should exhibit two different optoelectronic behaviors. The *J*-aggregation of [***H*-ImPV.(*Cy*-DAT)$_2$**] favors its emission properties (solid-state fluorescence quantum yield) and the *Foster* aggregation of ***H*-ImPV** supports its charge transport abilities (intermolecular overlaps). This has been illustrated by the fabrication of light-emitting devices based on films of ***H*-ImPV** and [***H*-ImPV.(*Cy*-DAT)$_2$**] sandwiched between two electrodes (see Figure 11b). Taking into account HOMO (−5.45 eV) and LUMO (−3.03 eV) level positions, electroluminescent diodes based on ***H*-ImPV** were fabricated using a system ITO/PEDOT−PSS (−5 eV) as an anode and calcium (−2.9 eV) as a cathode. From such electronic structures, it is believed that charge carrier injection may differ. The energetic barrier at the anodic interface is higher in OLEDs based on [***H*-ImPV.(*Cy*-DAT)$_2$**] than in those based on ***H*-ImPV**. Hole injection is then easier in ***H*-ImPV**. At the cathodic interface, electron injection from calcium is not limited by any energetic barrier in both cases. As a consequence, charge balance may be better in ***H*-ImPV** than in [***H*-ImPV.(*Cy*-DAT)$_2$**]. On this energetic basis, higher performances are expected from ***H*-ImPV**. The structure of the device included a 50-nm-thick layer of poly(styrene sulfonate)-doped poly(3,4-ethylene dioxythiophene) (PEDOT-PSS) spun on indium tin oxide (ITO).[22] Then, the active layers of ***H*-ImPV** or [***H*-ImPV.(*Cy*-DAT)$_2$**] were deposited. The low solubility of the different modules in commonly used solvents for device fabrication prohibited spin-coating deposition. An alternative was found in the coevaporation of the chromophore and the structuring module under vacuum (ca. 10^{-6} mbar). This approach has recently been exploited by Fasel and Müllen for the deposition of heteromolecular assemblies of PTCDI (perylene tetracarboxylicdiimide) and 1,4-bisdiaminotriazinebenzene on a gold substrate.[23] Using scanning tunneling microscopy, they nicely demonstrated that heteromolecular supramolecular structures could result from the coevaporation of complementary building blocks through one-dimensional (1D) multitopic hydrogen-bonding interactions. In this context, ***H*-ImPV** and ***Cy*-DAT** were disposed in individual Al_2O_3 crucibles, and the flow rates were controlled by slowly increasing the temperature of each oven to reach the desired 1:2 ***H*-ImPV:*Cy*-DAT** stoichiometry. Experimentally, the flow rate of the structuring unit (***Cy*-DAT**) was first tuned before closing the corresponding oven by a shutter. The flow rate of the fluorophore was subsequently calibrated before opening both ovens. Finally, after checking that the total flow was the sum of the two contributions, the shutter of the substrate holder was opened. The deposited thicknesses (50 nm) were monitored using a piezoelectric balance setup inside the vacuum chamber close to the substrate holder. A cathode composed of calcium (∼100 nm thick) was then sublimed on the devices.

Figure 12a shows the measured intensity−luminance−voltage (*IVL*) characteristics of devices based on ***H*-ImPV** and on [***H*-ImPV.(Cy-DAT)$_2$**]. OLEDs based on [***H*-ImPV.(Cy-DAT)$_2$**] exhibited good luminance levels for voltages of <15 V (190 Cd/m^2 at 14.5 V) and the onset voltage is 8.5 V. An onset voltage of 12 V is recorded with devices based on ***H*-ImPV** and much smaller luminances for the same current density. Values of only 2.5 Cd/m^2 are observed at 15 V. Such very high applied voltages are consistent with poor performances of ***H*-ImPV**-based devices. As a consequence, the injection-related data reported above are not sufficient to predict the performance of OLEDs. We believe that ***H*-ImPV** presents a poor ability to emit light, because of its aggregation, which induces quenching of luminescence. Therefore, the use of ***Cy*-DAT** is an interesting alternative to avoid aggregation and to significantly increase luminance. As a consequence, the luminous efficiencies of the devices are much better for the coassembled active layer (see Figure 12b). Finally, tuning of the supramolecular organization of the ***H*-ImPV** by the addition of two equivalents of ***Cy*-DAT** in the active layer allowed to recover the performances exhibited by OLEDs of the chromophore covalently link to steric hindered groups, such as a triethoxysilane (**(*EtO*)$_3$-*Si*-ImPV**) or a cyclohexyl (***Cy*-ImPV**).[6] The good efficiencies exhibited by the devices based on a single layer of /[***H*-ImPV.(Cy-DAT)$_2$**] are the result of the *J*-aggregation of

(22) Wantz, G.; Hirsch, L.; Huby, N.; Vignau, L.; Silvain, J. F.; Barrière, A.-S.; Parneix, J.-P. *Thin Solid Films* **2005**, *485*, 247.

(23) Canas-Ventura, M. E.; Xiao, W.; Wasserfallen, D.; Müllen, K.; Brune, H.; Barth, J. V.; Fasel, R. *Angew. Chem., Int. Ed.* **2007**, *46*, 1814.

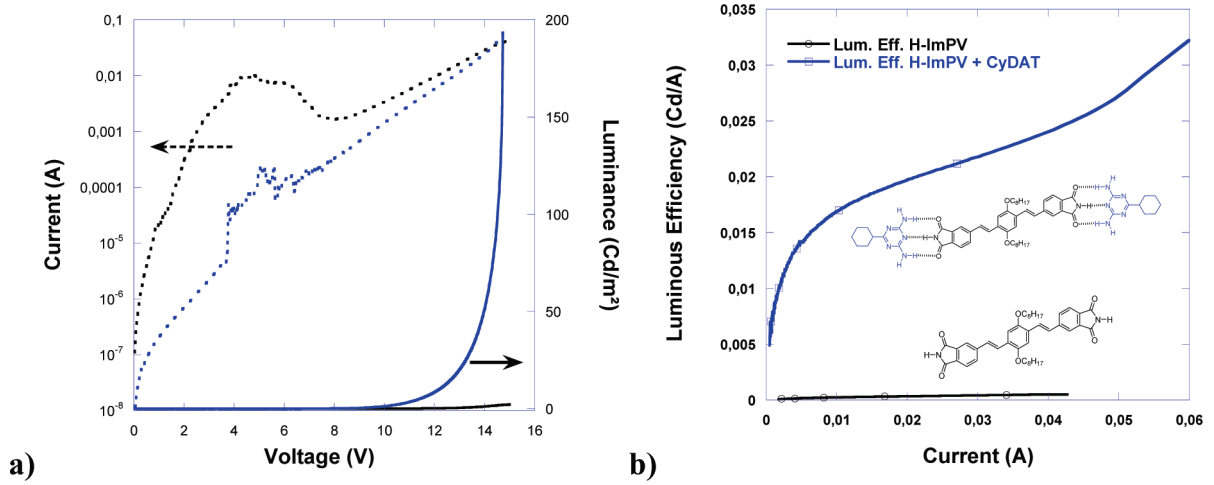

Figure 12. Performance of ITO/PEDOT-PSS/***H*-ImPV** (50 nm thick)/Ca (black curve) and ITO/PEDOT-PSS/[***H*-ImPV.(Cy-DAT)$_2$**] (50 nm thick)/Ca (blue curve) devices: (a) intensity−luminance−voltage (*IVL*) curves and (b) luminous efficiencies.

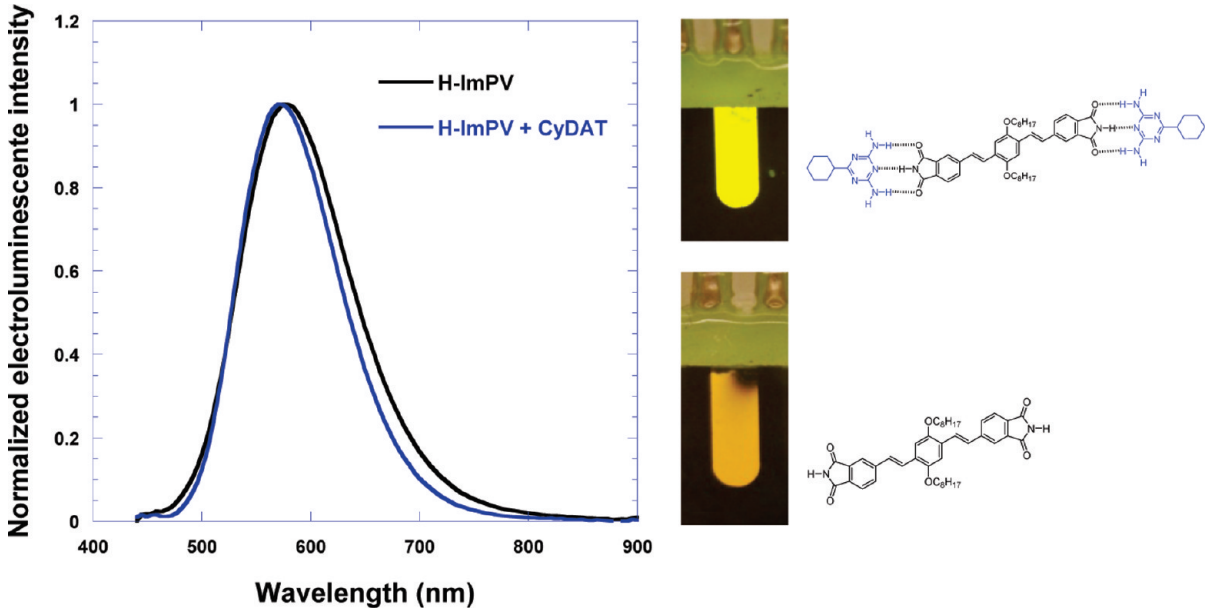

Figure 13. Electroluminescence (EL) spectra of ITO/PEDOT-PSS/***H*-ImPV** (50 nm thick)/Ca/Al (black curve) and ITO/PEDOT-PSS/[***H*-ImPV.(Cy-DAT)$_2$**] (50 nm thick)/Ca/Al (blue curve) devices.

chromophores directed by the bulky cyclohexyl fragments of the ***Cy*-DAT**.

The electroluminescence (EL) spectra have been measured and found centered at 575 nm with an onset at λ_{onset} = 495 nm for ***H*-ImPV** and at 570 nm with a onset at λ_{onset} = 503 nm for [***H*-ImPV.(*Cy*-DAT)$_2$**]. (See Figure 13.) Those EL spectra are in good agreement with the HOMO and LUMO level positions deduced by cyclic voltammetry, since it provides bandgap widths of 2.50 and 2.46 eV. As in the case of the photoluminescence of the films or powders, the observed light is yellow in the case of [***H*-ImPV.(*Cy*-DAT)$_2$**]-based OLEDs and red for ***H*-ImPV**-based OLEDs. Even if the chromatic coordinates, respectively calculated at $x = 0.47/y = 0.51$ and $x = 0.48/y = 0.50$ are quite similar, the ***H*-ImPV** device appeared redder than the two-component diode, because of its higher full width at half-maximum (fwhm). A red-shift is also observed on the EL spectra (see Figure 10, $\Delta\lambda = 20$ nm), compared to the photoluminescence spectrum of the chromophore. Such an effect related to built-in electric fields has already been observed.[24]

Fourier transform infrared spectroscopy−attenuated total reflectance (FT-IR−ATR) measurements realized on coevaporated films confirmed the contribution of the imide group to the formation of heteromolecular association. The infrared spectrum of [***H*-ImPV.(Cy-DAT)$_2$**], relative to ***H*-ImPV**, exhibited both shifting of the symmetric stretching band (ν_s(C═O)) to lower wavenumber ($\Delta\nu = -5\ cm^{-1}$) and shifting of the asymmetric stretching band (ν_{as}(C═O)) to higher wavenumber ($\Delta\nu = 5\ cm^{-1}$) (see Figure 14b). Those shifts are indicative of a more effective hydrogen bond in the triplet ADA···DAD.

(24) (a) Campbell, I. H.; Hagler, T. W.; Smith, D. L.; Ferraris, J. P. *Phys. Rev. Lett.* **1996**, *76*, 1900. (b) Bolognesi, A.; Bajo, G.; Paloheimo, J.; Östergärd, T.; Stubb, H. *Adv. Mater.* **1997**, *9*, 121.

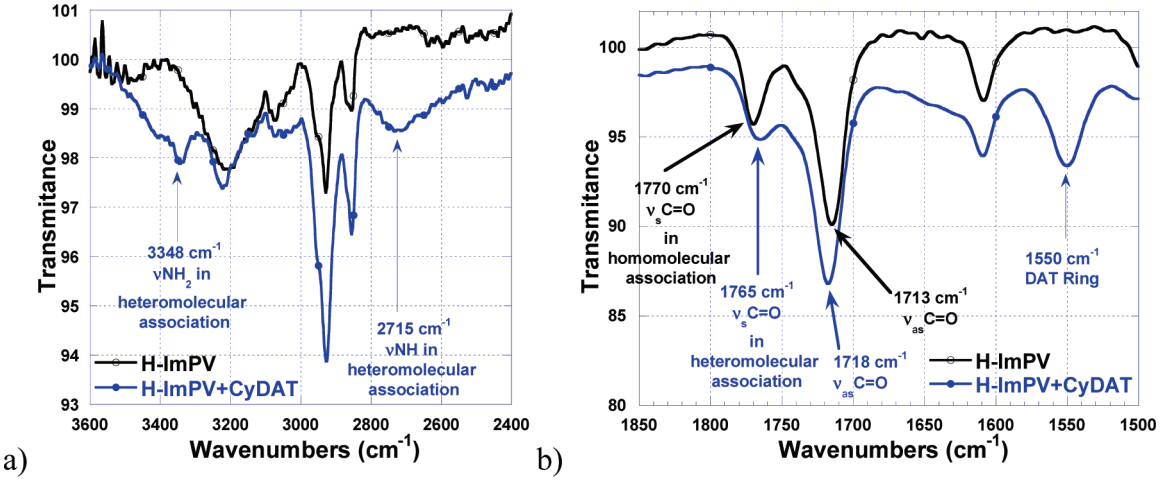

Figure 14. Fourier transform infrared spectroscopy−attenuated total reflectance (FT-IR−ATR) spectra of ***H*-ImPV** (50 nm thick) and [***H*-ImPV.(Cy-DAT)$_2$**] (50 nm thick) films evaporated on quartz substrates: (a) the N−H and C−H stretching mode region, and (b) the C=O stretching, the NH_2 bending, and in-plane triazine ring mode regions.

The band at ca. 2715 cm^{-1} assigned to N−H· · ·N interassociation of ***Cy*-DAT** and ***H*-ImPV** units is again clearly seen in the spectrum of the [***H*-ImPV.(Cy-DAT)$_2$**] film shown in Figure 14a.

Conclusion

In summary, we have developed a new strategy to tune the aggregation of a chromophore without any covalent modifications. For that purpose, a linear ditopic chromophore ***H*-ImPV** was synthesized. This N−H imide constitutes a recognizing unit with the acceptor−donor−acceptor (ADA) hydrogen bond motif. End-capping of this new chromophore with a monotopic structuring module (***Cy*-DAT**) bringing a steric hindrance allowed the control of its supramolecular aggregation. The studies of the absorption and emission properties of the ***H*-ImPV**, in solution or in the solid state (thin films, powders), clearly revealed different aggregation behaviors, depending on the presence of the monotopic structuring module (***Cy*-DAT**). In all cases, the signature of the heteromolecular association ***H*-ImPV**· · ·***Cy*-DAT** was evidenced by an infrared absorption band located at 2715 cm^{-1}, typical of the hydrogen bonding present in the ADA· · ·DAD triplet. This has been illustrated by the fabrication of light-emitting devices based on films of ***H*-ImPV** and [***H*-ImPV.(*Cy*-DAT)$_2$**]. ***H*-ImPV** presents a poor ability to emit light, because of its aggregation, which induces quenching of luminescence. The good efficiencies exhibited by the devices based on a single layer of [***H*-ImPV.(Cy-DAT)$_2$**] are the result of the *J*-aggregation of chromophores directed by the bulky cyclohexyl fragments of the ***Cy*-DAT**. Tuning of the supramolecular organization of the ***H*-ImPV** via the addition of 2 equiv of ***Cy*-DAT** in the active layer allowed recovery of the performances exhibited by OLEDs of the chromophore covalently link to steric hindered group such as a triethoxysilane or a cyclohexyl. The use of ***Cy*-DAT** seems to be a more interesting alternative to avoid aggregation and significantly increase luminance. We believe that this approach of the control of electro-optical properties by the control of aggregation properties could be generalized to many labile and versatile structure-directing groups. As a consequence, the luminous efficiencies of the devices are much better for the coassembled active layer. Such a strategy applied on multilayer and highly efficient OLEDs should allow new display solutions to be developed.

We are currently working on the transfer of this plug-and-play strategy to wet processes. In particular, spin-coating-processed light-emitting diodes are under investigation and will be reported in due course.

Acknowledgment. The authors gratefully acknowledge financial support from the "Ministère de la Recherche" and the CNRS. This work was supported by the ANR-07-JCJC-0022 grant/NANOTECTUM and the TRIMATEC competitiveness cluster. We are grateful to Prof. Rute Sa Ferreira (University of Aveiro, Departmente of Physics and CICECO, Portugal) for the quantum yield measurements.

Supporting Information Available: Experimental procedure for the synthesis of ***H*-ImPV**, ***Cy*-DAT**, ***Cy*-DAT*Hex*$_4$**, and ***Ph*-DAT.** Spectral data sets (NMR, UV−vis, fluorescence and FTIR spectra, HRMS, elemental analyses) and ^{1}H and ^{13}C NMR spectra for ***H*-ImPV**, ***Cy*-DAT**, ***Cy*-DAT*Hex*$_4$**, and **Ph-DAT**. Determination protocol for association constants. Thin-films and device fabrication methods. This material is available free of charge via the Internet at http://pubs.acs.org.